Synthesis, crystal structure, antioxidation and DNA-binding properties of the Ln complexes with 1-phenyl-3-methyl-5-hydroxypyrazole-4-carbaldhyde-(benzoyl)hydrazone

Hong-Ge Li, Zheng-Yin Yang *, Bao-Dui Wang, Jin-Cai Wu

College of Chemistry and Chemical Engineering, State Key Laboratory of Applied Organic Chemistry, Lanzhou University, Lanzhou 730000, PR China

A B S T R A C T

Two lanthanide complexes (Ln = La, Pr) with a PMFP Schiff-base, 1-phenyl-3-methyl-5-hydroxypyrazole-4-carbaldhyde-(benzoyl)hydrazone (H_2L) were synthesized and characterized. The crystal structure of the La complex was determined by single-crystal X-ray diffraction, the coordination polyhedron is a tri-capped trigonal prism configuration with the nine-coordinate atoms composed of three nitrogens and six oxygens from three ligands. The complex crystallized in the monoclinic lattice with a space group $P2/c$. Electronic absorption titration spectra, fluorescence titration spectra, EtBr competitive experiment, viscosity measurement and CD spectra indicate that all the complexes can strongly bind calf thymus DNA, presumably via groove binding and intercalation mechanism. Furthermore, investigations of antioxidation properties show that all the complexes have some scavenging effects for hydroxyl radicals.

© 2009 Elsevier B.V. All rights reserved.

1. Introduction

It is well known that DNA is an important cellular receptor, many chemicals exert their antitumor effects through binding to DNA thereby changing the replication of DNA and inhibiting the growth of the tumor cells, which is the basis of designing new and more efficient antitumor drugs and their effectiveness depends on the mode and affinity of the binding [1–3]. Small molecules possess DNA-binding abilities include metal complexes, porphyrins, natural antibiotics, simple aromatic hydrocarbons and some heterocyclic cations [4–9]. Particularly, the DNA-binding metal complexes have been extensively studied as DNA structural probes, DNA-dependent electron transfer probes, DNA footprinting and sequence-specific cleaving agents and potential anticancer drugs [10–12]. Basically, metal complexes interact with the double helix DNA in either a non-covalent or a covalent way. The former way includes three binding modes: intercalation, groove binding and external static electronic effects. Among these interactions, groove binding is one of the most important DNA-binding modes as it invariably leads to cellular degradation.

As well as the magnetic and photophysical properties, the bioactivities of lanthanides such as antimicrobial, antitumor, antivirus, anticoagulant action, prevention from arteriosclerosis, etc., have been explored in recent decades [13–16]. In addition, some

Schiff-bases metal chelates have represented good antitumor activities against animal tumors [17,18].

Based on the above considerations, lanthanide complexes with Schiff-bases derived from PMBP and chromone have always been a major concern for our group [19–21]. In this paper, two lanthanide complexes (Ln = La, Pr) with a Schiff-base 1-phenyl-3-methyl-5-hydroxypyrazole-4-carbaldhyde-(benzoyl)hydrazone were synthesized and their DNA-binding modes were investigated.

On the other hand, reactive oxygen species (ROS) are generated by normal cellular metabolism and by exogenous agents. Even though ROS may serve as cell signaling or bactericidal agents, excess ROS can cause damage to cellular macromolecules such as polyun-saturated lipid, protein, and DNA, leading to a process called oxidative stress [22,23]. Oxidative stress is implicated in the development of many diseases such as macular degeneration, cardiacdisease, drug-associated toxicity, inflammation, atherogenesis and premature aging [24–26].

Since among all reactive oxygen species the hydroxyl radical is by far the most potent and therefore the most dangerous oxygen metabolite, elimination of this radical is one of the major aims of antioxidant administration. Although a variety of (OH·) scavengers are known, their application is limited by: (1) the requirement of unphysiologically high scavenger concentrations which depend on the rate constant, (2) toxic side effects including initiation of further radical chain reactions, or (3) the instability of the compound in biological systems [27]. Many researchers have been working hard to develop complexes in order to achieve the

efficient scavenger. It has been recently demonstrated that some minor groove binders for DNA are effective inhibitors of the formation of a DNA/TBP complex or topoisomerases [28,29]. The antioxidation properties of the lanthanide complexes were also investigated in this paper.

2. Experimental

2.1. Materials

All chemicals used were of analytical grade and used without further purification unless otherwise noted. Calf thymus DNA (CT-DNA) and ethidium bromide (EtBr) were obtained from Sigma–Aldrich Biotech. Co., Ltd. CT-DNA stock solution was prepared by dissolving the solid material, normally at 0.3 mg ml^{-1}, in 5 mM Tris–HCl buffer (pH 7.20) containing 50 mM NaCl. Whereafter, the solution was kept over 48 h at 4 °C. Calf thymus DNA (CT-DNA) obtained from Sigma. UV–Vis spectrometer was employed to check DNA purity 1.8–1.9:1 and concentration ($\varepsilon = 6600$ M^{-1} cm^{-1} at 260 nm) [30]. All the stock solutions (1.0 mMl) of the investigated compounds were prepared by dissolving the powder materials into appropriate amounts of DMF or CH$_3$OH solutions, respectively. Double-distilled water was used to prepare buffers.

2.2. Instrumentation and methods

The melting points of the compounds were determined on an XT4-100X microscopic melting point apparatus (Beijing, China). The IR spectra were recorded on a Therrno Mattson FT-IR spectrometer using KBr disc in the 4000–400 cm^{-1} region. ^{1}H NMR spectra were recorded on a Varian VR 300-MHz spectrometer with tetramethylsilane (TMS) as an internal standard. ESI-MS (ESI-Trap/Mass) spectra were recorded on a Bruker Esquire6000 Mass spectrophotometer.

The UV–Vis spectra were recorded on a Perkin–Elmer Lambda-35 UV–Vis (Ultraviolet and Visible) spectrophotometer. Absorption titration experiments were performed by maintaining the ligand and metal complexes concentration as constant at 10 μM while increasing the concentration of nucleic acid. While measuring the absorption spectra, equal quantity of CT-DNA was added to both the complex and the reference solution to eliminate the absorbance of DNA itself.

For fluorescence measurements, fixed amounts (10 μM) of the complexes were titrated with increasing amounts of CT-DNA. The excitation and emission wavelength were 332, 359 and 418, 474 nm for the ligand and two complexes, respectively. Excitation and emission slit were set at 5 nm. Experiments were conducted at room temperature in a buffer containing 5 mM Tris–HCl (pH 7.2) and 50 mM NaCl concentrations.

EtBr–DNA competitive experiment was performed as reported in a literature [31]. DNA (4.0 μM, nucleotides) solution was added incrementally to 0.32 μM EtBr solution, until the rise in the fluorescence ($\lambda_{ex} = 496$ nm, $\lambda_{em} = 596$ nm) attained a saturation. Then, small aliquots of concentrated compound solutions (1.0 mM) were added till the drop in fluorescence intensity ($\lambda_{ex} = 525$ nm, $\lambda_{em} = 589$ nm) reached a constant value. Measurements were made after 5 min at room temperature.

Viscosity titration experiments were carried on an Ubbelohde viscometer in a thermostated water-bath maintained at 25.00 ± 0.01 °C. DNA concentration was kept constant (5 μM) and gradually increased the concentration of tested compound (0.5–3.5 μM). Data were presented as $(\eta/\eta_0)^{1/3}$ vs. the ratio of the compound to DNA, where η is the viscosity of DNA in the presence of the compound corrected from the solvent effect, and η_0 is the viscosity of DNA alone. Relative viscosities for DNA in either the presence or absence of compound were calculated from the following relation [32,33].

$$\eta = (t - t_0)/t_0$$

where t is the observed flow time of the DNA containing solution, and t_0 is the flow time of buffer.

The CD spectra were recorded on an Olos RSM 1000 at increasing complex/DNA ratio ($r = 0.0$ and 1.0). Each sample solution was scanned in the range of 220–320 nm. A CD spectrum was generated which represented the average of two scans from which the buffer background had been subtracted. The concentration of DNA was 3.0×10^{-4} M.

The hydroxyl radicals (OH·) in aqueous media were generated through the Fenton-type reaction [34]. The solution of the tested compound was prepared with DMF. The 5 ml reaction mixtures contained 2 ml of 100 mM phosphate buffer (pH 7.4), 1.0 ml of 0.10 mM aqueous safranin, 1 ml of 1.0 mM aqueous EDTA–Fe(II), 1 ml of 3% aqueous H$_2$O$_2$, and a series of quantitatively microadding solutions of the tested compound. The sample without the tested compound was used as the control. The reaction mixtures were incubated at 37 °C for 60 min in a water-bath. The absorbances of the samples and a control were measured at 520 nm. The suppression ratio for OH· was calculated from the following Eq. (1) [35,36].

$$\text{Scavenging effect } (\%) = \frac{A_{sample} - A_{blank}}{A_{control} - A_{blank}} \times 100 \qquad (1)$$

where A_{sample} is the absorbance of the sample in the presence of the tested compound, A_{blank} is the absorbance of the blank in the absence of the tested compound and $A_{control}$ is the absorbance in the absence of the tested compound and EDTA–Fe (II). IC$_{50}$ value was introduced to denote the molar concentration of the tested compound which caused good inhibitory or scavenging effect on hydroxyl radicals.

2.3. X-ray crystallography

A yellow crystal of [La(HL)$_3$]·1.5(C$_2$H$_5$OH)·1.5(H$_2$O) was obtained by slow vapor diffusion of C$_2$H$_5$OH/ether at room temperature. X-ray diffraction data for the crystal were performed with graphite-monochromated Mo K radiation (0.71073 Å) on a Bruker APEX area-detector diffractometer and collected by the $\omega/2\theta$ scan technique at 298(2) K. The crystal structure was solved by direct methods. All non-hydrogen atoms were refined anisotropically by full-matrix least-squares methods on F^2. Primary non-hydrogen atoms were solved by direct method and secondary non-hydrogen atoms were solved by difference maps. The hydrogen atoms were added geometrically and not refined. All calculations were performed using the programs SHELXS-97 and SHELXL-97.

2.4. Preparation of ligand and its complexes

2.4.1. Synthesis of the ligand (H$_2$L)

The ligand of 1-phenyl-3-methyl-5-hydroxypyrazole-4-carbaldhyde-(benzoyl)hydrazone was prepared according to the literature [37].

2.4.2. Synthesis of lanthanide complexes

An ethanol solution containing the La nitrate (0.2 mM, 0.086 g) was added dropwise to a stirred yellow solution of ligand H$_2$L (0.35 mM, 0.112 g) in ethanol (40 ml) at 60 °C. After 12 h at this temperature, 20 ml distilled water was added dropwise to the reaction solution which was concentrated to 5 ml, immediately there was a yellow precipitate in the solution. The yellow precipitate was separated from the solution by suction filtration, purified

by washing several times with water, and dried for 48 h under vacuum. The Pr complex were prepared by the same method.

3. Results and discussion

3.1. Description of the crystal structure

On the basis of the single-crystal X-ray analysis of the complex [La(HL)$_3$]·1.5(C$_2$H$_5$OH)·1.5(H$_2$O), the La ion is located at the center of a tricapped trigonal prism configuration coordination environment, which consists of three nitrogens and six oxygens from three ligands. The complex crystallized in the monoclinic lattice with a space group P2/c. Each unit cell contained four molecules. The coordination sphere of ORTEP diagram is in Fig. 1, which presents a pseudo helix structure. The X-ray diffraction data for the La complex are given in Table 1 and the selected bond lengths and angles are summarized in Table 2.

Ligand H$_2$L acts as a tridentate ligand, binding to La through the oxygen atom of pyrazole ring (enolized and deprotonated from O=C−), and the C=N group, O=C group of the benzoylhydrazine side chain. The distance for C12−O2, C30−O4 and C48−O6 are 1.255 (Å), 1.264 (Å) and 1.276 (Å), respectively, which are between the C−O (1.410–1.440 Å) and C=O (1.19–1.23 Å) distances [38], this result shows that oxygen atoms of pyrazole ring of all three ligands take part in coordination by the enolic form, and their active hydrogen is replaced by La atom. But O=C group of the benzoylhydrazine side chain does not enolized, which can be demonstrated by bond lengths C7−O1 (1.234 Å), C25−O3 (1.238 Å) and C37−O5 (1.234 Å). Moreover, there are C$_2$H$_5$OH and H$_2$O solvent molecule in the lattice.

3.2. Infrared spectra

The main stretching frequencies of the IR spectra of the complexes are tabulated in Table 3. On the basis of the similar IR spectra of the two complexes, it may be assumed that they have similar coordination structures. The aqueous ν(OH) bands of La and Pr complexes appear at 3408, 3356 cm^{-1}. This shows that there is some crystal water in the complexes [33,39]. The ν(C=O)$_{(hydrazonic)}$
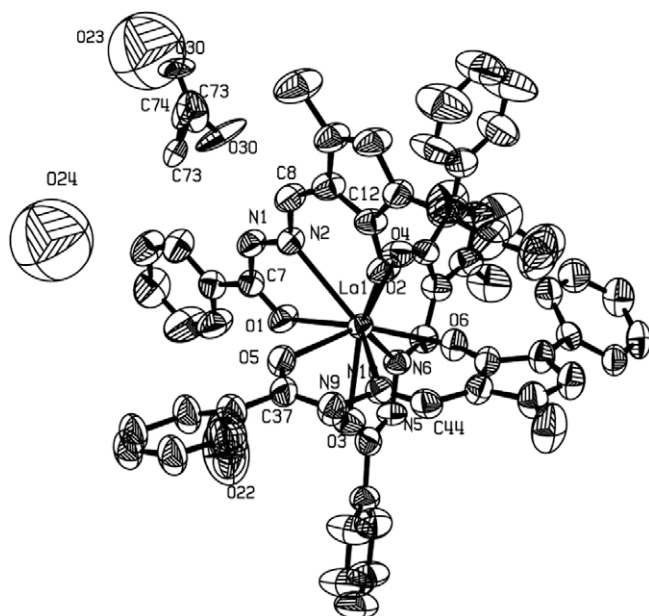
Fig. 1. Thermal ellipsoid diagram of [La(HL)$_3$]·1.5(C$_2$H$_5$OH)·1.5(H$_2$O). Hydrogen atoms have been excluded for clarity.

Table 1
Crystallographic data and structure refinement for the La complex.

Empirical formula	C$_{57}$H$_{54}$LaN$_{12}$O$_9$
Formula weight	1190.03
Crystal colour	Yellow
Crystal size (mm)	0.31 × 0.27 × 0.25
T (K)	296(2)
Wavelength (Å)	0.71073
Crystal system	Monoclinic
Space group	P2/c
a (Å)	13.1407(5)
b (Å)	11.5427(4)
c (Å)	0.6615(14)
α (°)	90
b (°)	90.675(2)
g (°)	90
V (Å^3)	6167.1(4)
Z	4
D$_{Calc}$ (Mg/m^3)	1.282
Absorption coefficient (mm^{-1})	0.797
F(0 0 0)	2504
θ Range (°)	0.989–24.10
Reflections collected/unique [R$_{int}$]	29 129/9679 [0.0567]
Goodness-of-fit on F^2	1.015
R indices [I > 2σ(I)]	R$_1$ = 0.0774, wR$_2$ = 0.2272

vibrations of the free ligand is at 1656 cm^{-1} but for the two complexes these peaks shift to about 1618 cm^{-1}. The band at 1591 cm^{-1} for the free ligand is assignable to the ν(C=N) stretch, which shifts to 1567 and 1569 cm^{-1} for La and Pr complexes. Weak bands are observed at 417 and 430 cm^{-1}. These low frequency bands indicate the Ln ion and nitrogen and/or oxygen ligands.

3.3. Biological activities

3.3.1. Electronic absorption spectroscopy

The application of electronic absorption spectroscopy in DNA-binding studies is one of the most useful techniques [40]. To clarify the interactions between the compounds and DNA, the electronic absorption spectra of the ligand and its Ln complexes (Ln = La, Pr) in the absence and in the presence of the CT-DNA (at a constant concentration of the compounds) were obtained, which are shown in Fig. 2, respectively. With increasing DNA concentrations, the absorption bands at 239 nm and 342 nm of the ligand represent hypochromism of 15.60% and 14.66%; the absorption bands at 240 nm and 358 nm of the La complex exhibit hypochromism of 23.06% and 23.66%; the absorption bands at 242 nm and 362 nm of the Pr complex appear hypochromism of 22.33% and 21.50%. The hypochromism observed for the $\pi\rightarrow\pi^*$ transition bands indicating strong binding of the ligand and complexes to DNA. The absorption data were analyzed to evaluate the intrinsic binding constant K_b, which can be determined from Eq. (2) [41].

$$[DNA]/(\varepsilon_a - \varepsilon_f) = [DNA]/(\varepsilon_b - \varepsilon_f) + 1/[K_b(\varepsilon_b - \varepsilon_f)] \quad (2)$$

where [DNA] is the concentration of DNA in base pairs; ε_a, ε_f and ε_b is the apparent extinction coefficient (A_{obsd}/[compound]), the extinction coefficient for free compound and the extinction, respectively, coefficient for compound in the fully bound form. In plots of [DNA]/($\varepsilon_a - \varepsilon_f$) vs. [DNA], K_b is given by the ratio of the slope to the intercept. K_b values of the ligand, La and Pr complexes were 2.29 × 10^4 M^{-1}, 1.50 × 10^5 M^{-1} and 5.01 × 10^4 M^{-1}, respectively, which were consist with hypochromism degree. The K_b values obtained here are lower than that reported for classical intercalator (for ethidium bromide and [Ru(phen)DPPZ] whose binding constants have been found to be in the order of 10^6–10^7 M^{-1}) [42–45]. It is clear that the hypochromism and K_b values are not enough evidence, but these results can suggest an intimate association of

Table 2
Selected bond lengths and angles.

O(6)–La(1)–O(4)	78.0(2)	O(2)–La(1)–N(6)	143.4(2)	C(7)–O(1)–La(1)	127.1(5)
O(6)–La(1)–O(2)	80.4(2)	O(5)–La(1)–N(6)	128.6(2)	C(12)–O(2)–La(1)	135.9(5)
O(4)–La(1)–O(2)	83.0(2)	O(3)–La(1)–N(6)	59.0(2)	C(25)–O(3)–La(1)	126.9(6)
O(6)–La(1)–O(5)	130.87(19)	O(1)–La(1)–N(6)	76.1(2)	C(30)–O(4)–La(1)	133.9(6)
O(4)–La(1)–O(5)	147.1(2)	N(10)–La(1)–N(6)	116.7(2)	C(37)–O(5)–La(1)	125.5(6)
O(2)–La(1)–O(5)	86.9(2)	N(2)–La(1)–N(6)	122.7(2)	C(48)–O(6)–La(1)	135.0(5)
O(6)–La(1)–O(3)	86.7(2)	C(10)–N(3)–N(4)	108.0(7)	O(1)–C(7)–N(1)	121.2(8)
O(4)–La(1)–O(3)	130.1(2)	C(12)–N(4)–N(3)	109.9(7)	O(1)–C(7)–C(6)	119.9(8)
O(2)–La(1)–O(3)	140.9(2)	C(12)–N(4)–C(13)	128.5(7)	N(1)–C(7)–C(6)	118.9(8)
O(5)–La(1)–O(3)	74.2(2)	N(3)–N(4)–C(13)	121.6(7)	N(2)–C(8)–C(9)	123.2(8)
O(6)–La(1)–O(1)	145.2(2)	C(25)–N(5)–N(6)	118.3(8)	N(3)–C(10)–C(9)	110.2(8)
O(4)–La(1)–O(1)	86.7(2)	C(25)–N(5)–H(5A)	120.8	N(3)–C(10)–C(11)	121.2(9)
O(2)–La(1)–O(1)	128.84(19)	N(6)–N(5)–H(5A)	120.8	O(2)–C(12)–N(4)	123.0(8)
O(5)–La(1)–O(1)	75.6(2)	C(26)–N(6)–N(5)	115.3(7)	O(2)–C(12)–C(9)	130.9(8)
O(3)–La(1)–O(1)	79.6(2)	C(26)–N(6)–La(1)	129.9(6)	N(4)–C(12)–C(9)	106.1(7)
O(6)–La(1)–N(10)	70.60(19)	N(5)–N(6)–La(1)	114.0(5)	C(14)–C(13)–N(4)	120.8(9)
O(4)–La(1)–N(10)	140.7(2)	C(28)–N(7)–N(8)	105.1(8)	C(14)–C(13)–C(18)	119.2(10)
O(2)–La(1)–N(10)	69.1(2)	C(30)–N(8)–C(31)	131.2(8)	N(4)–C(13)–C(18)	120.0(9)
O(5)–La(1)–N(10)	60.5(2)	C(30)–N(8)–N(7)	109.0(8)	O(3)–C(25)–N(5)	121.2(9)
O(3)–La(1)–N(10)	71.8(2)	C(31)–N(8)–N(7)	119.2(8)	O(3)–C(25)–C(24)	119.5(9)
O(1)–La(1)–N(10)	132.4(2)	C(37)–N(9)–N(10)	116.8(7)	N(5)–C(25)–C(24)	119.3(9)
O(6)–La(1)–N(2)	139.9(2)	C(37)–N(9)–H(9A)	121.6	N(6)–C(26)–C(27)	122.8(8)
O(4)–La(1)–N(2)	72.2(2)	N(10)–N(9)–H(9A)	121.6	N(9)–C(37)–C(38)	116.8(9)
O(2)–La(1)–N(2)	70.00(19)	C(44)–N(10)–N(9)	114.3(7)	N(10)–C(44)–C(45)	123.4(8)
O(5)–La(1)–N(2)	74.9(2)	C(44)–N(10)–La(1)	131.1(6)	N(11)–C(46)–C(45)	111.2(8)
O(3)–La(1)–N(2)	133.2(2)	N(9)–N(10)–La(1)	114.3(5)	N(11)–C(46)–C(47)	121.0(9)
O(1)–La(1)–N(2)	59.15(18)	C(46)–N(11)–N(12)	105.6(7)	O(6)–C(48)–N(12)	122.6(8)
N(10)–La(1)–N(2)	119.7(2)	C(48)–N(12)–N(11)	111.2(7)	O(6)–C(48)–C(45)	130.8(8)
O(6)–La(1)–N(6)	69.4(2)	C(48)–N(12)–C(49)	127.9(7)	O(30)–C(74)–O(30)#1	132(2)
O(4)–La(1)–N(6)	71.2(2)	N(11)–N(12)–C(49)	120.6(7)	O(30)–C(74)–C(73)	87.5(14)

Table 3
Some main IR data of the ligand and its complexes.

Compound	$v(OH)$	$v(NH)$	$v(C=O)$	$v(C=N)$	$v(M–N)$
H₂L		3116m	1656w	1591s	
[La(HL)₃]	3408w	3062m	1618s	1567s	417w
[Pr(HL)₃]	3343w	3061m	1618s	1569s	430w

the compounds with CT-DNA and indicate that the binding strength of complex is in the order of La complex > Pr complex > H₂L.

3.3.2. Fluorescence spectroscopy

Fixed amounts (10 μM) of the complexes were titrated with increasing amounts of CT-DNA. The fluorescence titrations spectra of complexes in the absence and presence of CT-DNA are given in Fig. 3. Compared to the complexes alone, the fluorescence intensity of the complexes are quenched steadily with the increasing concentration of the CT-DNA. This phenomenon of the quenching of luminescence of the complex by DNA may be attributed to the photoelectron transfer from the guanine base of DNA to the excited MLCT state of the complex [46–51]. These changes also proved that there were conjugation functions between CT-DNA and compounds. [52,53].

3.3.3. Competition experiment

In order to further investigate the interaction mode between the complexes and CT-DNA, the ethidium bromide (EtBr) fluorescence competitive experiments were also employed. The intrinsic fluorescence intensity of DNA is very low, and that of EtBr in Tris–HCl buffer is also not high due to the quenching by the solvent molecules. However, on addition of DNA, the fluorescence intensity of EtBr will be enhanced because of its intercalation into the DNA. However, the enhanced fluorescence can be quenched evidently when there is a second molecule that can replace DNA-bound EtBr (if it binds to DNA more strongly than EtBr) and/or accept the excited state electron from EtBr [54,55], or possibly break the second-

ary structure of DNA [56]. Therefore, EtBr can be used to probe the interaction of complexes with DNA. Fig. 4 shows the emission spectra of DNA–EtBr system with increasing amounts of the complexes. The emission intensity of the DNA–EtBr system (λ_{em} = 589 nm) decreased apparently as the concentration of complexes increased, and the quenching plots illustrate that the quenching of EtBr bound to DNA by the complexes is in good agreement with the linear Stern–Volmer equation [57].

$$F_0/F = 1 + K_q[Q] \tag{3}$$

where F_0 and F are the fluorescence intensity in the absence and in the presence of compound at $[Q]$ concentration, respectively; K_q is the quenching rate constant. The shape of Eq. (3) plots can be used to characterize the quenching as being predominantly dynamic or static.

Insert figure in Fig. 4 show the plots of F_0/F vs. $[Q]$. The data of K_q are all at 10^4 M^{-1} level for ligand, La and Pr complexes, accordingly. In view of the strong interaction of EtBr with DNA of which the binding constant of EtBr with DNA is at 10^6 M^{-1} level [43], we consider it is impossible for the complexes to scramble EtBr from DNA. Similar fluorescence quenching effect of EtBr bound to DNA has been observed for the addition of several groove-binding compounds, including netropsin and distamycin A [58,59]. The observed results make us to suspect that the complex may interact with DNA through the groove binding mode or intercalation mode, releasing some EtBr molecules from EtBr–DNA system [59–61].

3.3.4. Viscosity studies

Viscosity titration measurements were carried out to further clarify the interaction modes between the investigated compounds and CT-DNA. Hydrodynamic measurements that are sensitive to changes in the length of DNA (i.e. viscosity and sedimentation) are regarded as the least ambiguous and the most critical tests of binding in solution in the absence of crystallographic structural data [11]. The classic intercalation model involves the insertion of a planar molecule between DNA base pairs, which results in a
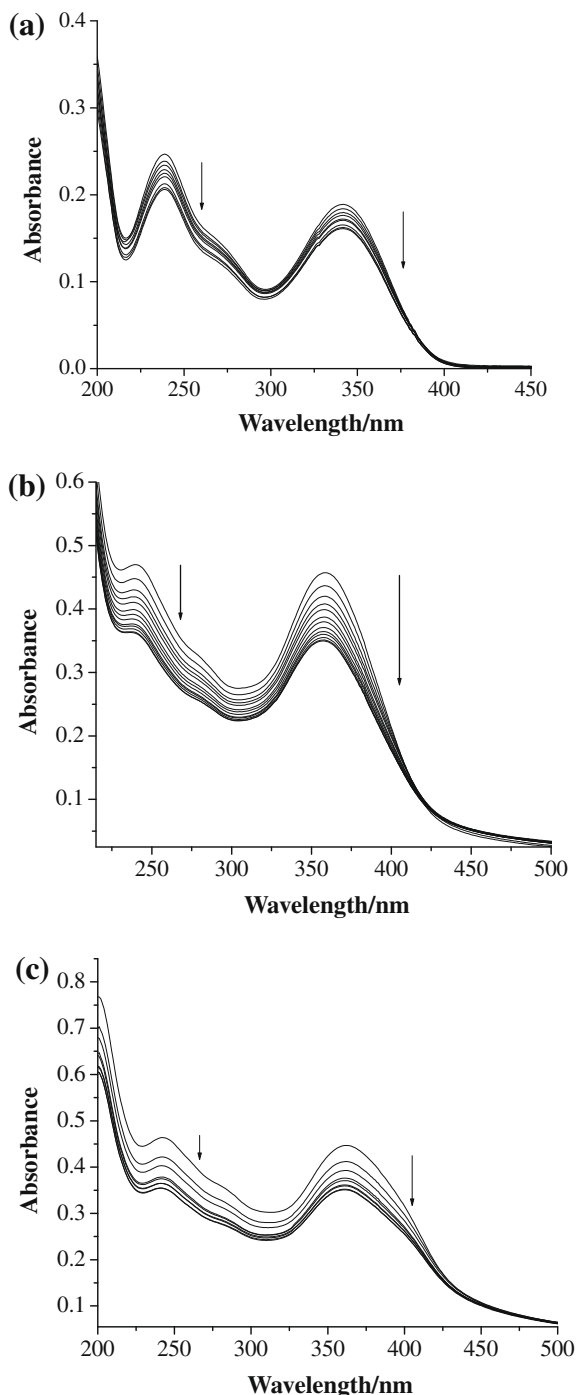
Fig. 2. (a) Electronic spectra of the ligand (10 μM) in the presence of CT-DNA. [DNA] = 0–18 μM. Arrow shows the absorbance changes upon increasing DNA concentration. (b) Electronic spectra of the La complex (10 μM) in the presence of CT-DNA. [DNA] = 0–20 μM. Arrow shows the absorbance changes upon increasing DNA concentration. (c) Electronic spectra of the Pr complex (10 μM) in the presence of CT-DNA. [DNA] = 0–24 μM. Arrow shows the absorbance changes upon increasing DNA concentration.

Fig. 3. (a) The emission enhancement spectra of the ligand (10 μM) in the presence of 0–20 μM CT-DNA. Arrow shows the emission intensities changes upon increasing DNA concentration. (b) The emission enhancement spectra of the La complex (10 μM) in the presence of 0–25 μM CT-DNA. Arrow shows the emission intensities changes upon increasing DNA concentration. (c) The emission enhancement spectra of the Pr complex (10 μM) in the presence of 0–17.5 μM CT-DNA. Arrow shows the emission intensities changes upon increasing DNA concentration.

decrease in the DNA helical twist and lengthening of the DNA, the molecule will be in close proximity to the DNA base pairs as well [32,62,63]. In contrast, molecule that binds exclusively in the DNA grooves by partial and/or non-classical intercalation, under the same conditions, typically cause less pronounced (positive or negative) or no change in DNA solution viscosity [35,64]. The effects of the compounds on the viscosity of rod-like DNA at 25.00 ± 0.01 °C are shown in Fig. 5. With the ratios of the investi-

gated compounds to DNA (bps) increasing, the relative viscosities of DNA first increased and then decreased, may indicating that these compounds can bind to DNA by groove mode and intercalation mode [65,66]. The changed degree of viscosity which follows the order of La complex > Pr complex > H₂L, may depend on its affinity to DNA, which is consistent with electronic absorption spectroscopy studies. In addition, the viscosity changes of the Ln (Ln = La, Pr) salts are far small than those of Schiff-base complexes. The higher binding affinity of the complexes is probably relate to its helix structure since the structure of the La complex is able to
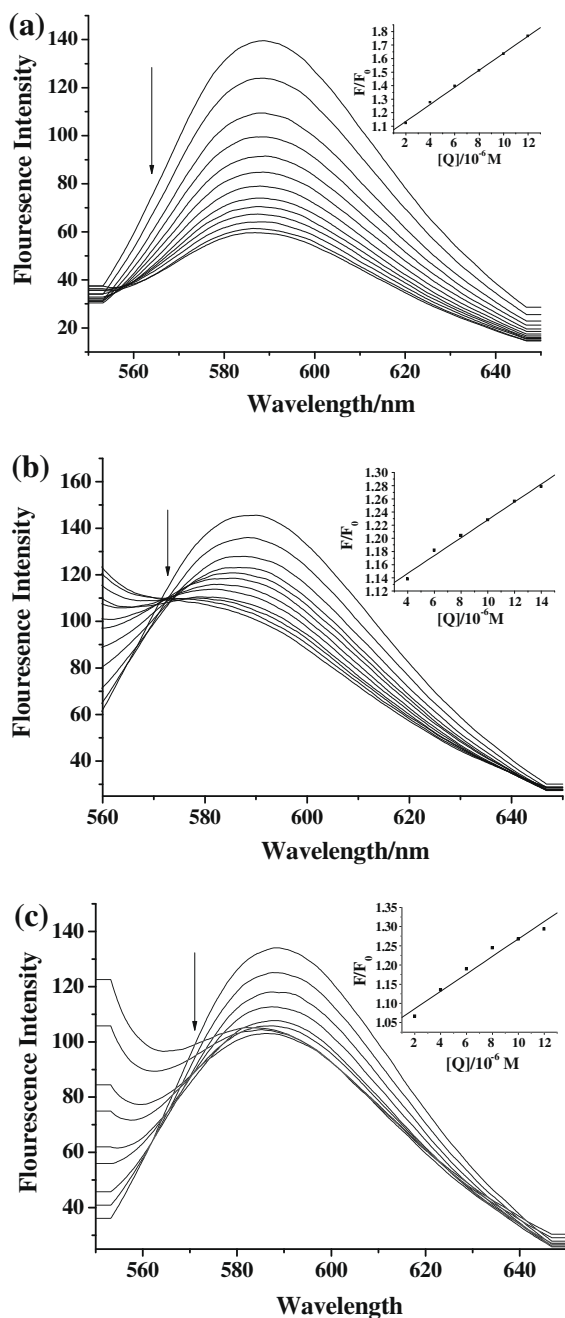
Fig. 4. (a) The emission spectra of calf thymus DNA–EtBr system in the presence of 0–30 μM the ligand. Arrow shows the emission intensities changes upon increasing ligand concentration. (Inset) Stern–Volmer plot of the fluorescence titration data of ligand. (b) The emission spectra of calf thymus DNA–EtBr system in the presence of 0–27.5 μM La complex. Arrow shows the emission intensities changes upon increasing ligand concentration. (Inset) Stern–Volmer plot of the fluorescence titration data of La complex. (c) The emission spectra of calf thymus DNA–EtBr system in the presence of 0–20 μM Pr complex. Arrow shows the emission intensities changes upon increasing ligand concentration. (Inset) Stern–Volmer plot of the fluorescence titration data of Pr complex.

provide lots of grooving positions to stack more strongly with the base pairs of the DNA helix [58].

3.3.5. Circular dichroism (CD) studies

Circular dichroic spectral technique is useful in diagnosing changes in DNA morphology during drug–DNA interactions, as the band due to base stacking (275 nm) and that due to right-handed helicity (248 nm) are quite sensitive to the mode of DNA
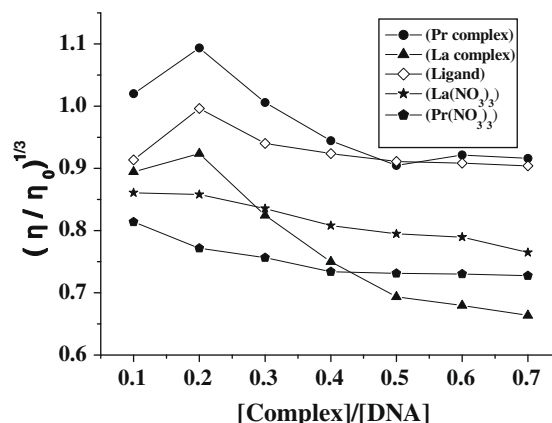
Fig. 5. Effect of increasing amounts of the ligand, Ln complex and Ln (Ln = La, Pr) salts on the relative viscosity of CT-DNA at 25.00 ± 0.01 °C.

interactions with small molecules [67]. The changes in CD signals of DNA observed on interaction with drugs may often be assigned to the corresponding changes in DNA structure [68]. The circular dichroic spectrum of CT-DNA (Fig. 6) exhibits a positive band at 270 nm and a negative band at 243 nm, and both bands increased in intensity upon addition of the La complex to DNA. This phenomenon may be due to the intercalation of the complex through p-stacking which stabilizes the right-handed B form DNA [47].

3.3.6. Hydroxyl radical scavenging activity

Generation of reactive oxygen species (ROS) is a normal process in the life of aerobic organisms. It has been estimated that free radical-induced DNA damage in humans is at biologically relevant levels, with approximately 10^4 DNA bases being oxidatively modified per cell per day. Oxidative damage to DNA has been suggested to contribute to aging and various diseases including cancer and chronic inflammation [69]. Since among all reactive oxygen species, the hydroxyl radical (OH$^\cdot$) is by far the most potent and therefore the most dangerous oxygen metabolite, elimination of this radical is one of the major aims of antioxidant administration [70]. Consequently, in this paper, the ligand and its Ln complexes (Ln = La, Pr) studied for their antioxidant activity by comparing their scavenging effects on hydroxyl radical (OH$^\cdot$).

Fig. 7 shows the plots of hydroxyl radical scavenging effects (%) for the ligand, Ln complexes and Ln salts (Ln = La, Pr). The values of
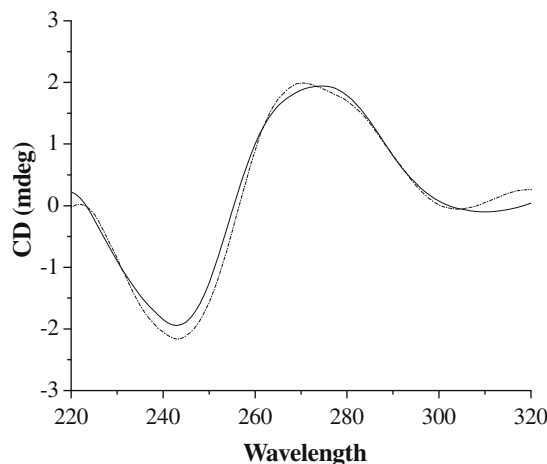
Fig. 6. CD spectra of CT-DNA in the absence (Solid line) and presence (Dash Dot line) of La complex at r = 1.0 (r = molar ratio [compound]/[CT-DNA]).
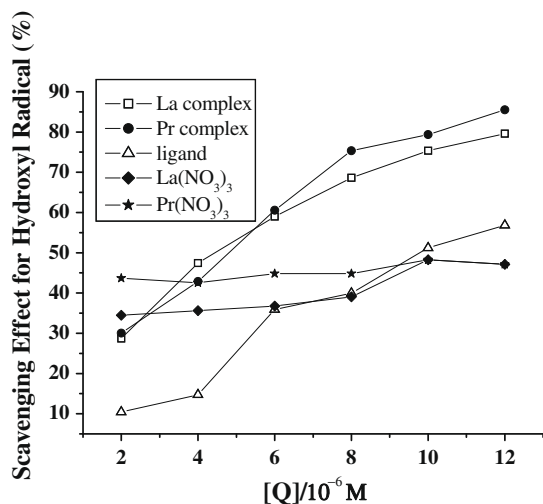
Fig. 7. Plots of the hydroxyl radical scavenging effects (%) for the ligand, Ln complexes and Ln (Ln = La, Pr) salts, respectively.

IC_{50} of ligand and coplexes for hydroxyl radical scavenging effects are 10.13 μM, 5.01 μM and 4.883 μM, respectively, with the order of Pr complex < La complex < H_2L. It is proved that the hydroxyl radical scavenging effects of Ln complexes are much higher than that of the ligand. Moreover, the values of IC_{50} of La and Pr salts for hydroxyl radical scavenging effects are 13.61 μM and 16.72 μM, so the hydroxyl radical scavenging effects (%) for Ln (Ln = La, Pr) salts are weaker than those of the corresponding complexes and the ligand.

4. Conclusions

In summary, a PMFP Schiff-base ligand, 1-phenyl-3-methyl-5-hydroxypyrazole -4-carbaldhyde-(benzoyl)hydrazone (H_2L) and its two lanthanide complexes (Ln = La, Pr) have been prepared and characterized. Furthermore, the DNA-binding properties of the ligand and its lanthanide complex were investigated by spectra titration and viscosity measurements. Experimental results indicate that the complexes can bind to CT-DNA both via the mode of groove binding and intercalation, and two complexes have stronger binding affinity than the ligand. On the other hand, the ligand and two lanthanide complexes all have some abilities of antioxidation for hydroxyl radicals but two lanthanide complexes show stronger scavenging effects for hydroxyl radicals than ligands. These findings clearly indicate that lanthanide complexes with PMFP Schiff-base have many potential practical applications. However, their pharmacodynamical, pharmacological and toxicological properties should be further studied in vivo.

Acknowledgement

Appendix A. Supplementary material

CCDC 732414 contain the supplementary crystallographic data for this paper. These data can be obtained free of charge from The Cambridge Crystallographic Data Centre via www.ccdc.cam.ac.uk/data_request/cif. Supplementary data associated with this article can be found, in the online version, at doi:10.1016/j.jorganchem.2009.10.032.

References

[1] J.K. Barton, J.M. Goldberg, C.V. Kumar, N.J. Turro, J. Am. Chem. Soc. 108 (1986) 2081.
[2] A.M. Pyle, T. Morii, J.K. Barton, J. Am. Chem. Soc. 112 (1990) 9432.
[3] Y.B. Zeng, N. Yang, W.S. Liu, N. Tang, J. Inorg. Biochem. 97 (2003) 258.
[4] Y. An, Y.Y. Lin, H. Wang, H.Z. Sun, M.L. Tong, L.N. Ji, Z.W. Mao, Dalton Trans. 12 (2007) 1250.
[5] T. Kobayashi, S. Tobita, M. Kobayashi, T. Imajyo, M. Chikira, M. Yashiro, Y. Fujii, J. Inorg. Biochem. 101 (2007) 348.
[6] B. Chen, S. Wu, A. Li, F. Liang, X. Zhou, X. Cao, Z. He, Tetrahedron 62 (2006) 5487.
[7] C.Y. Wei, G.Q. Jia, J.L. Yuan, Z.C. Feng, C. Li, Biochemistry 45 (2006) 6681.
[8] A.A. Ghazaryan, Y.B. Dalyan, S.G. Haroutiunian, A. Tikhomirova, N. Taulier, J.W. Wells, T.V. Chalikian, J. Am. Chem. Soc. 128 (2006) 1914.
[9] F.Y. Wu, F.Y. Xie, Y.M. Wu, J.I. Hong, J. Fluoresc. 18 (2008) 175.
[10] Y. Xiong, L.N. Ji, Coord. Chem. Rev. 185 (1999) 711.
[11] D.S. Sigman, A. Mazumder, D.M. Perrin, Chem. Rev. 93 (1993) 2295.
[12] C. Metcalfe, J.A. Thomas, Chem. Soc. Rev. 32 (2003) 215.
[13] M. Albrecht, O. Osetska, R. Fröhliich, Dalton Trans. 23 (2005) 3757.
[14] D. Parker, R.S. Dickins, H. Puschmann, C. Crossland, J.A.K. Howard, Chem. Rev. 102 (2002) 1977.
[15] R.B. Hunter, W. Walker, Nature 178 (1956) 47.
[16] D.M. Kramsch, A.J. Aspen, L.J. Rozler, Science 213 (1981) 1511.
[17] E.M. Hodnett, W.J. Dunn, J. Med. Chem. 15 (1972) 339.
[18] E.M. Hodnett, P.D. Mooney, J. Med. Chem. 13 (1970) 786.
[19] Y. Wang, Z.Y. Yang, Transit. Met. Chem. 30 (2005) 902.
[20] Z.Y. Yang, Y. Wang, Y. Wang, Bioorg. Med. Chem. Lett. 17 (2007) 2096.
[21] B.D. Wang, Z.Y. Yang, T.R. Li, Bioorg. Med. Chem. 14 (2006) 6012.
[22] B. Halliwell, J.M.C. Gutteridge, Oxford Science Publications, New York. 1999, p. 936.
[23] B. Halliwell, Annu. Rev. Nutr. 16 (1996) 33.
[24] B.N. Ames, M.K. Shigenaga, T.M. Hagen, Proc. Natl. Acad. Sci. USA 90 (1993) 7915.
[25] A.A. Horton, S. Fairhurst, Crit. Rev. Toxicol. 18 (1987) 27.
[26] H.L. Wang, Z.Y. Yang, B.D. Wang, Transit. Met. Chem. 31 (2006) 470.
[27] J.G. Wu, R.W. Deng, Z.N. Chen, Transit. Met. Chem. 18 (1993) 23.
[28] S.Y. Chiang, J. Welch, F.J. Rauscher, T.A. Beerman, Biochemistry 33 (1994) 7033.
[29] A.Y. Chen, C. Yu, B. Gatto, L.F. Liu, Proc. Natl. Acad. Sci. USA 90 (1993) 8131.
[30] C.V. Kumar, E.H. Asuncion, J. Am. Chem. Soc. 115 (1993) 8547.
[31] A.G. Krishna, D.V. Kumar, B.M. Khan, S.K. Rawal, K.N. Ganesh, Biochim. Biophys. Acta 1381 (1998) 104.
[32] D. Suh, J.B. Chaires, Bioorg. Med. Chem. 3 (1995) 723.
[33] S. Satyanarayana, J.C. Dabrowiak, J.B. Chaires, Biochemistry 31 (1992) 9319.
[34] C.C. Winterbourn, Biochem. J. 198 (1981) 125.
[35] B.D. Wang, Z.Y. Yang, P. Crewdson, D.Q. Wang, J. Inorg. Biochem. 101 (2007) 1492.
[36] Z.Y. Guo, R.E. Xing, S. Liu, H.H. Yu, P.B. Wang, C.P. Li, P.C. Li, Bioorg. Med. Chem. Lett. 15 (2005) 4600.
[37] H.G. Li, Z.Y. Yang, D.D. Qin, Inorg. Chem. Commun. 12 (2009) 494.
[38] X.M. Chen, J.W. Cai (Eds.), Single-Crystal Structural Analysis. Principles and Practices, Science Press, Beijing, 2003.
[39] Z.Y. Yang, Synth. React. Inorg. Met-Org. Chem. 30 (2000) 1265.
[40] J.K. Barton, A.T. Danishefsky, J.M. Goldberg, J. Am. Chem. Soc. 106 (1984) 2172.
[41] A. Wolfe, G.H. Shimer, T. Meehan, Biochemistry 26 (1987) 6392.
[42] M. Cory, D.D. McKee, J. Kagan, D.W. Henry, J.A. Miller, J. Am. Chem. Soc. 107 (1985) 2528.
[43] M.J. Waring, J. Mol. Biol. 13 (1965) 269.
[44] V.G. Vaidyanathan, B.U. Nair, J. Inorg. Biochem. 94 (2003) 121.
[45] R. Vijayalakshmi, M. Kanthimathi, V. Subramanian, B.U. Nair, Biochim. Biophys. Acta 1475 (2000) 157.
[46] R. Vijayalakshmi, M. Kanthimathi, R. Parthasarathi, B.U. Nair, Bioorg. Med. Chem. 14 (2006) 3300.
[47] P.U. Maheswari, M. Palaniandavar, J. Inorg. Biochem. 98 (2004) 219.
[48] A.K. Mesmaeker, G. Orellana, J.K. Barton, N.J. Turro, Photochem. Photobiol. 52 (1990) 461.
[49] J.B. Chaires, N. Dattagupta, D.M. Crothers, Biochemistry 21 (1982) 3933.
[50] J.Z. Wu, L. Yuan, J.F. Wu, J. Inorg. Biochem. 99 (2005) 2211.
[51] B. Peng, H. Chao, B. Sun, H. Li, F. Gao, L.N. Ji, J. Inorg. Biochem. 101 (2007) 404.
[52] P.X. Xi, Z.H. Xu, F.J. Cheng, Z.Z. Zeng, X.W. Zhang, J. Inorg. Biochem. 103 (2009) 210.
[53] P.X. Xi, Z.H. Xu, X.H. Liu, F.J. Cheng, Z.Z. Zeng, Spectrochim Acta A 71 (2008) 523.
[54] R. Indumathy, S. Radhika, M. Kanthimathi, T. Weyhermuller, B.U. Nair, J. Inorg. Biochem. 101 (2007) 434.
[55] B. Selvakumar, V. Rajendiran, P.U. Maheswari, H. Stoeckli-Evans, M. Palaniandavar, J. Inorg. Biochem. 100 (2006) 316.
[56] M. Chauhan, F. Arjmand, J. Organomet. Chem. 692 (2007) 5156.
[57] M.R. Efink, C.A. Ghiron, Anal. Biochem. 114 (1981) 199.
[58] Z.Y. Yang, B.D. Wang, Y.H. Li, J. Organomet. Chem. 691 (2006) 4159.
[59] S.M. Nelson, L.R. Ferguson, W.A. Denny, Mutat. Res. 623 (2007) 24.
[60] D.L. Boger, B.E. Fink, S.R. Brunette, W.C. Tse, M.P. Hedrick, J. Am. Chem. Soc. 123 (2001) 5878.
[61] Z.Q. Liu, M. Jiang, Y.T. Li, Z.Y. Wu, J.X. Yang, Inorg. Chim. Acta 362 (2009) 1253.
[62] R. Palchaudhuri, P.J. Hergenrother, Curr. Opin. Biotechnol. 18 (2007) 497.
[63] L.S. Lerman, J. Mol. Biol 3 (1961) 18.

[64] T.M. Kelly, A.B. Tossi, D.J. McConnell, T.C. Strekas, Nucleic Acids Res. 13 (1985) 6017.
[65] S. Mahadevan, M. Palaniandavar, Inorg. Chem. 37 (1998) 693.
[66] P.T. Selvi, M. Palaniandavar, Inorg. Chim. Acta 337 (2002) 420.
[67] V.I. Ivanov, L.E. Minchenkova, A.K. Shchelkina, A.I. Poletaev, Biopolymers 12 (1973) 89.
[68] P. Lincoln, E. Tuite, B. Norden, J. Am. Chem. Soc. 119 (1997) 1454.
[69] K. Tsai, T.G. Hsu, K.M. Hsu, H. Cheng, T.Y. Liu, C.F. Hsu, C.W. Kong, Free Radical Biol. Med. 31 (2001) 1465.
[70] N. Udilova, A.V. Kozlov, W. Bieberschulte, K. Frei, K. Ehrenberger, H. Nohl, Biochem. Pharm. 65 (2003) 59.